Synthesis of Conjugated Polyrotaxanes

Jasper J. Michels,[a] Michael J. O'Connell,[a] Peter N. Taylor,[a] Joanne S. Wilson,[b] Franco Cacialli,[c] and Harry L. Anderson*[a]

Abstract: A series of conjugated polyrotaxane insulated molecular wires are synthesised by aqueous Suzuki polymerisation, using hydrophobic binding to promote threading of the cyclodextrin units. These polyrotaxanes have conjugated polymer cores based on poly(*para*-phenylene), polyfluorene, and poly(diphenylene-vinylene), threaded through 0.9–1.6 cyclodextrins per repeat unit. Bulky naphthalene-3,6-disulfonate endgroups prevent the macrocycles from slipping off the conjugated polymer chains. Dialysis experiments show that the cyclodextrins become unthreaded only if smaller stoppers are used. MALDI TOF mass spectra detect oligomers with up to ten threaded cyclodextrins, and reveal the presence of some defects that result for oxidative homo-coupling of boronic acids. Weight-average molecular weights were determined by analytical ultracentrifugation, demonstrating that step-growth polymerisation is efficient enough to achieve degrees of polymerisation up to ≈20 repeat units (84 *para*-phenylenes). The fluorescence spectra

Keywords: cyclodextrins · nanotechnology · rotaxanes · self-assembly · supramolecular chemistry

of these polyrotaxanes indicate that the presence of the threaded cyclodextrin macrocycles reduces the flexibility of the conjugated polymer π-systems. Both the solution and the solid-state photoluminescence quantum yields are enhanced upon threading of the conjugated polyaromatic cores through α- or β-cyclodextrins, and the emission spectra of the polyrotaxanes are blue-shifted compared to the corresponding unthreaded polymers. The greater weight of the 0–0 transition in the emission spectra, as well as the smaller Stokes shift, indicate that the polyrotaxanes are more rigid than the unthreaded polymers.

Introduction

Conjugated polymers have attracted widespread interest due to their applications in light-emitting diodes,[1] field-effect transistors[2] and photovoltaic devices.[3] They are often loosely described as *molecular wires* because of the high charge-mobility along individual polymer chains.[4]

[a] Dr. H. L. Anderson, Dr. J. J. Michels, M. J. O'Connell, Dr. P. N. Taylor
Department of Chemistry, University of Oxford
Dyson Perrins Laboratory, South Parks Road, Oxford, OX1 3QY (UK)
Fax: (+44) 1865-275-674
E-mail: harry.anderson@chem.ox.ac.uk

[b] Dr. J. S. Wilson
Department of Physics, University of Cambridge
Cavendish Laboratory
Madingley Road, Cambridge, CB3 0HE (UK)

[c] Dr. F. Cacialli
Department of Physics and Astronomy, University College London
Gower Street, London, WC1E 6BT (UK)

Supporting information for this article is available on the WWW under http://www.chemeurj.org/ or from the author. This includes synthetic procedures and spectroscopic data for monomers **4a–6**, and crystallographic data for **4b** and **4c**.

However, inter-chain charge-mobilities can also be fairly high,[5] and π–π stacking interactions between polymer chains can dramatically affect the optical behaviour, for example, by broadening the absorption and emission spectra and quenching the fluorescence.[6] This makes it interesting to study *insulated molecular wires* in which the conjugated polymer backbone is encapsulated at the molecular level by a protective sheath, limiting inter-chain interactions and enhancing the one-dimensional nature of the transport properties. Encapsulation can enhance the chemical stability[7] and luminescent efficiency[8] of the conjugated core. When exploiting the electronic functionality of single molecules it is important to prevent cross-talk, and the design of molecularly isolated conducting structures may enable the size of electronic circuits to be reduced to molecular dimensions.[9] Insulated molecular wires have been created by threading conjugated polymers through cyclophanes,[10,11] cyclodextrins[12] and zeolites,[9,13] by wrapping them in polymer helices,[14] and by decorating them with dendritic side-chains.[15] Here, we present some polyrotaxanes[16] consisting of a conjugated polymer core threaded through a series of cyclodextrin macrocycles.[17] Although many polyrotaxanes have been reported,[18] and there are several examples of conjugated poly-pseudorotaxanes,[11,12] to the best of our knowledge the ma-

terials reported here are the first genuine conjugated polyro-
taxanes with bulky endgroups preventing the macrocycles
from slipping off the chain.[17] This kinetic stability, with re-
spect to unthreading, is vital for purification and solution
processing.

   We report the synthesis and chemical characterisation of
four water-soluble conjugated polyrotaxanes: $1 \subset \beta$-CD, $2 \subset \beta$-
CD, $3 \subset \alpha$-CD and $3 \subset \beta$-CD (Figure 1), based on poly-*para*-
phenylene (PPP), polyfluorene (PF) and polydiphenylene-
vinylene (PDV) respectively, which illustrates the broad
scope of this synthetic approach. The molecular weights of
these polymers were determined by analytical ultracentrifu-
gation. In the case of $1 \subset \beta$-CD, it also proved possible to
probe the degree of polymerisation by MALDI-TOF MS
and GPC. We prove that these insulated wires are true ro-
taxanes by testing for unthreading during dialysis as a func-
tion of the size of the endgroup. The absorption and emis-
sion spectra as well as luminescence efficiencies of the poly-
rotaxane are compared to those of the uninsulated wires.
Encapsulation was found to enhance the luminescence effi-
ciency and shifted the emission to shorter wavelengths.

Results and Discussion

Synthesis and purification of polyrotaxanes: Our general
route to conjugated polyrotaxanes is an A+B step-growth
polymerisation, as outlined in Scheme 1. The hydrophobic
monomer (diboronic acid **5a–c**) is non-covalently bound
inside the macrocycle (α- or β-cyclodextrin) and polymer-
ised by Suzuki coupling[19] with a water-soluble monomer
(diiodide **4a–c**) to form a polypseudorotaxane. Finally, the
chains are terminated with bulky stoppers (iodonaphthalene
6) to prevent the macrocycles from slipping off the conjugat-
ed core. This whole sequence of reactions is carried out in
one pot, in an aqueous solution, and hydrophobic binding is
used to drive the threading process. The structures of the
components are summarised in Table 1.[20] Diboronic glycol
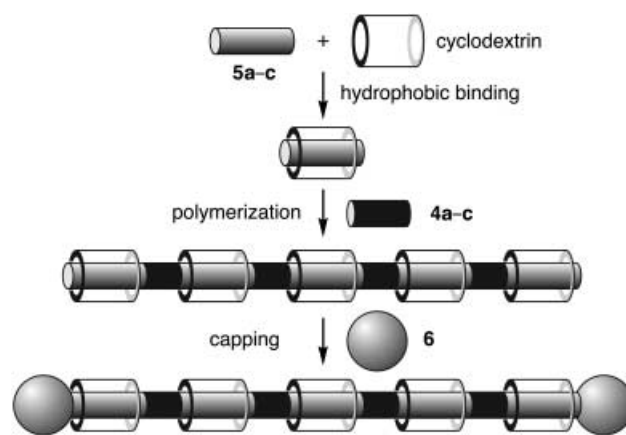
Scheme 1. Synthesis of polyrotaxanes; polymerisation and capping are
aqueous Suzuki couplings.

esters **5a–c** were used instead of free boronic acids to facili-
tate monomer purification. Suzuki polymerisations were car-
ried out at 85°C in aqueous lithium carbonate (0.17 M)
under nitrogen. Similar polymers are obtained by running
the reaction at 45°C, but a higher temperature was generally
used to ensure complete polymerisation and to increase the
solubility of the cyclodextrin. We employed palladium(II)
acetate as the catalyst precursor, without adding phosphine
ligands.[21] A polymerisation stoichiometry of **4a–c**:**5a–
c**:**6**:Pd:CD = 1:(1+a/2+b):a:b:4.0, was used to give a 1:1
ratio of the two bifunctional monomers after some diboronic
acid has coupled to the stopper **6** and some has undergone
homo-coupling[22] reducing the Pd^{II} to the active Pd^0 species
(evidence for this homo-coupling is provided by the
MALDI-TOF mass spectra discussed below). The predicted
number-average degree of polymerisation, $\bar{n}_{Nom}$ (Figure 1)
can be calculated from the endgroup-to-monomer ratio (a)
with the simple equation $\bar{n}_{Nom} = 2/a$, assuming that the
Suzuki coupling reaction goes cleanly to completion, and ne-
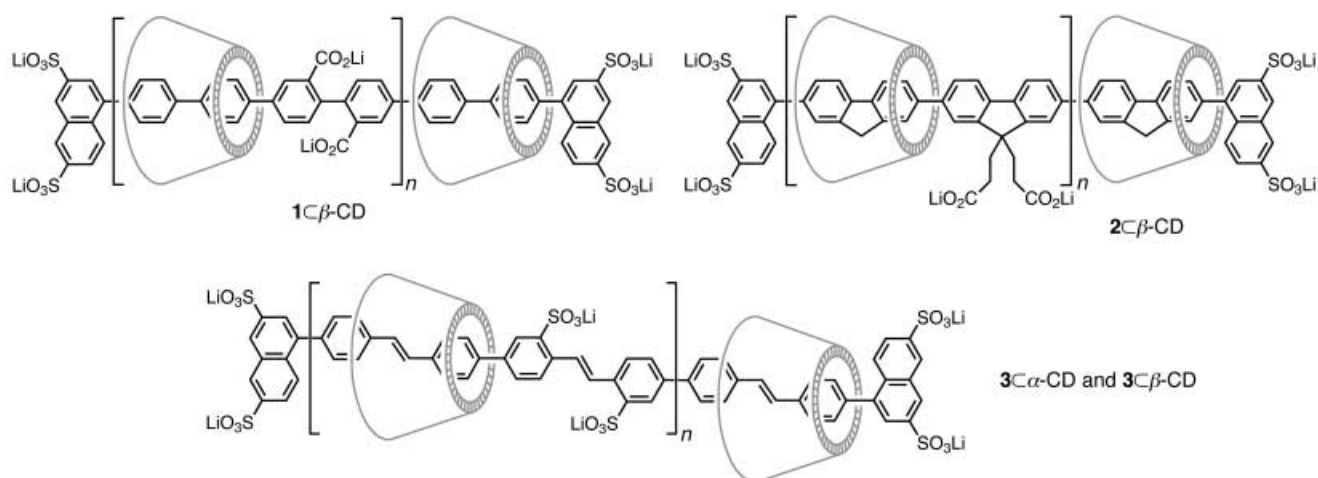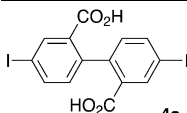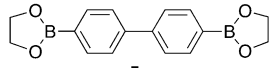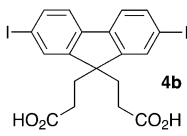glecting homo-coupling. Generally, we produced polyrotax-
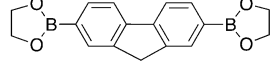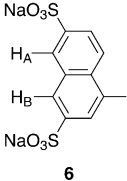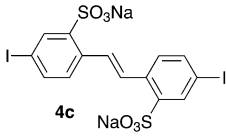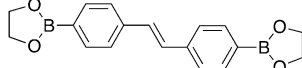
Figure 1. Idealised structures of the four polyrotaxanes studied in this work. Note that these materials are polydisperse in two respects: each has a range
of chain lengths (n) and a range of cyclodextrin loadings. The relative orientation of cyclodextrins on each chain is probably random. When referring to
these polymers we generally include the nominal stoichiometry-predicted number-average degree of polymerisation, for example, $\bar{n}_{Nom} = 10$.

Table 1. Structures of component monomers and macrocycles for polyrotaxane synthesis.[20]

Diiodide	Diboronic	Endgroup	Macrocycle	Polyrotaxane	Polymer Backbone
4a	**5a**		β-CD	**1**$\subset\beta$-CD	poly(para-phenylene) PPP
4b	**5b**	**6**	β-CD	**2**$\subset\beta$-CD	poly(fluorene) PF
4c	**5c**		α-CD β-CD	**3**$\subset\alpha$-CD **3**$\subset\beta$-CD	poly(diphenylene vinylene) PDV

anes with $\bar{n}_{\text{Nom}} = 10$ by the use of an endgroup-to-monomer ratio of $a = 0.2$. In the next section we show that these predicted degrees of polymerisation compare well with experimental values from analytical ultracentrifugation. Generally, we used 10 mol% palladium catalyst ($b = 0.1$), although similar results were also obtained with 3 mol% palladium. With the PPP and PF polyrotaxanes, only β-cyclodextrin was used to complex the aromatic core, whereas PDV-based polyrotaxanes were produced with threaded α- and β-cyclodextrin because stilbene units are slim enough to bind inside the narrower α-cyclodextrin cavity.

Excess cyclodextrin was removed from the crude polycarboxylate polyrotaxanes **1**$\subset\beta$-CD and **2**$\subset\beta$-CD by precipitation with acid and centrifugation. Redissolving the precipitate in aqueous lithium carbonate and ultrafiltration through a membrane with a nominal molecular weight cut-off (NMWCO) of 5 kDa removed low molecular weight material, including any remaining unthreaded cyclodextrin. The PDV-based rotaxanes **3**$\subset\alpha$-CD and **3**$\subset\beta$-CD were not precipitated with acid on account of the low pK_a of the sulfonic acid residues. In these cases, free cyclodextrin was removed by ultrafiltration. The crude products are generally contaminated with colloidal palladium catalyst residues, which are too coarse to be removed by ultrafiltration and too fine to be removed by a 0.1 μm filter. Several methods were tested for the removal of these palladium particles. Dithiocarbamates have been found to be effective for dissolving palladium,[23] so we tested N-dithiocarboxy glycine as a water-soluble dithiocarbonate; however, it was ineffective at dissolving these colloids. Fortunately, cyanide was found to be very effective. When aqueous alkaline solutions of the crude polyrotaxanes are treated with sodium cyanide, in the presence of air, the solutions change from grey to clear in about five minutes as the palladium dissolves to form $Na_2[Pd(CN)_4]$, which is removed by ultrafiltration. Analysis of the samples before and after treatment with cyanide showed that the wt% Pd decreased from 0.6% to <0.02%. Polymers **1**[$\bar{n}_{\text{Nom}} = 10$], **2**[$\bar{n}_{\text{Nom}} = 10$] and **3**[$\bar{n}_{\text{Nom}} = 10$] were synthesised and purified as reference compounds using identical procedures.

Polyrotaxane characterisation: *NMR and dialysis experiments*: A typical ^{1}H NMR spectrum of **1**$\subset\beta$-CD[$\bar{n}_{\text{Nom}} = 10$] is shown in Figure 2. Although the spectrum is poorly resolved, the ratio of the cyclodextrin and aromatic components can readily be determined by integration. The small
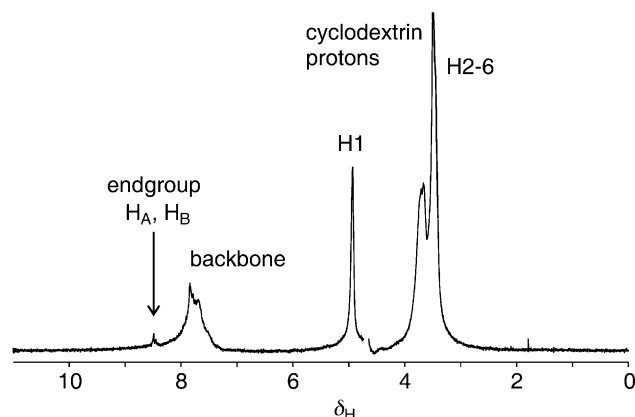

Figure 2. ^{1}H NMR (250 MHz, D_2O) spectrum of **1**$\subset\beta$-CD[$\bar{n} = 10$], $T = 20\,°C$ (a residual HOD signal at $\delta = 4.8$ ppm has been deleted).

signal at $\delta \approx 8.5$ ppm is assigned to protons H_A and H_B of the naphthalene disulfonate endgroups (see Table 1; this assignment is based on 2D NMR studies on the related [2]rotaxane[17a]). Integration of these endgroup signals provides experimental values for the number-average degree of polymerisation $\bar{n}_{\text{Nom}}$, which compare well with values from the polymerisation stoichiometry, $\bar{n}_{\text{Nom}}$, as shown in Table 2. In general, endgroup integration is an unreliable method of molecular weight determination because accidental termination or incomplete coupling[24] can result in chains with unexpected termini. However, with these polyrotaxanes, the fact that the cyclodextrins do not slip off the polymer backbones proves that the great majority of chains are terminated with bulky naphthalene stoppers, as shown below. The ^{1}H NMR spectra of the reference polymers **1**–**3** are broader

Table 2. Molecular weight parameters for polyrotaxanes and reference polymers.[a]

Polymer	$\bar{n}_{Nom}$	$\bar{y}_{NMR}$	$\bar{n}_{NMR}$	$\bar{M}_W$(calcd)	$\bar{v}$[mLg^{-1}]	$\bar{M}_W$ (AUC)	$\bar{n}_{AUC}$
1⊂βCD	10	1.1	7.7	34700	0.61	36800	10.6
2⊂βCD	10	1.1	10.5	36400	0.66	27100	7.3
3⊂αCD	10	0.9	7.9	29500	0.61	25800	8.7
3⊂βCD	10	1.6	7.7	49300	0.62	53500	10.9
1	10	0	11	8540	0.62	13900	16.6
2	10	0	–	10200	0.65	22500	22.8
3	10	0	–	11100	0.55	13400	12.1

[a] $\bar{n}_{Nom}$ is the stoichiometry-predicted number-average degree of polymerisation; $\bar{y}_{NMR}$ is the number-average threading ratio determined by ^{1}H NMR, $\pm 10\%$; $\bar{n}_{NMR}$ is the number-average degree of polymerisation from endgroup integration, $\pm 10\%$ for the polyrotaxanes and $\pm 20\%$ for **1**; $\bar{M}_W$ (calcd) is the weight-average molecular mass calculated from $\bar{n}_{Nom}$ and $\bar{y}_{NMR}$; $\bar{v}$ is the partial specific volume from oscillating capillary densitometry, $\pm 2\%$; $\bar{M}_W$ (AUC) is the weight-average molecular mass from analytical ultracentrifugation $\pm 10\%$; $\bar{n}_{AUC}$ is the average degree of polymerisation calculated from $\bar{M}_W$ (AUC) and $\bar{y}_{NMR}$, with an uncertainty of $\pm 10\%$.

than those of the polyrotaxanes (probably as a result of aggregation), making endgroup integration less reliable with **1** and impossible with **2** and **3**.

The polyrotaxanes are shown in Figure 1 with one threaded cyclodextrin per unsubstituted biphenyl, fluorene or stilbene unit. We define the *threading ratio* as $y = x/(n + 1)$, as shown in Figure 3, so this idealised representation corresponds to a threading ratio of $y = 1$. The threading ratio of each batch of polyrotaxane was determined by integration of the aromatic and cyclodextrin ^{1}H NMR signals to give the values listed in Table 2. All of the polyrotaxanes have threading ratios of $\bar{y}_{NMR} = 1.0 \pm 0.1$, except for **3**⊂$\beta$-CD, where the higher threading ratio ($\bar{y}_{NMR} = 1.6$) indicates that two β-cyclodextrins are quite easily accommodated on the unsubstituted stilbene unit.

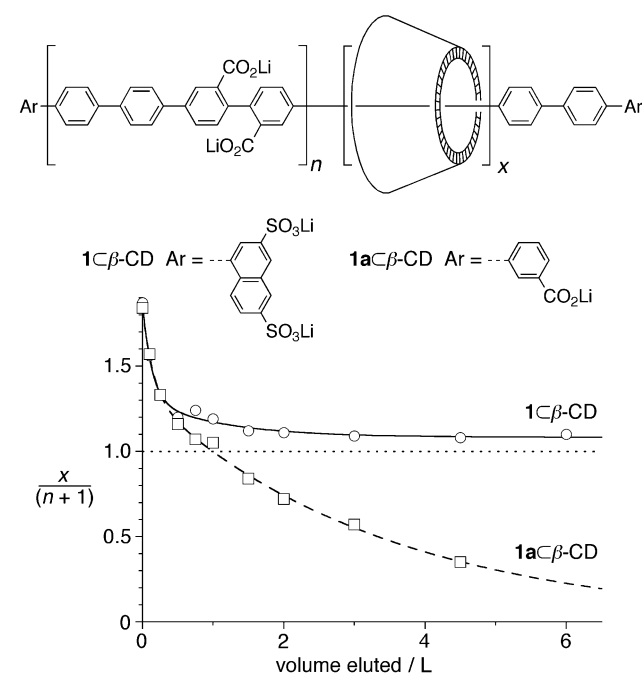To confirm that the naphthalene disulfonate endgroups are bulky enough to retain β-cyclodextrin, we tested wheth-

Figure 3. Plot of threading ratio from ^{1}H NMR integration [$\bar{y}_{NMR} = x/(n + 1)$] versus volume of water eluted during dialysis, with a 5 kDa NMWCO membrane using polyrotaxane **1**⊂β-CD and pseudopolyrotaxane **1a**⊂β-CD, both with $\bar{n}_{Nom} = 10$.

er unthreading occurs during dialysis. Two versions of poly-*para*-phenylene polyrotaxane were synthesised, one with large naphthalene disulfonate endgroups, **1**⊂β-CD[$\bar{n}_{Nom} = 10$], and one with small *meta*-benzoic acid terminals **1a**⊂β-CD[$\bar{n}_{Nom} = 10$] (Figure 3). The crude polyrotaxane reaction mixture (which initially contained excess cyclodextrin) was dialyzed with a 5 kDa NMWCO membrane. The threading ratio, $\bar{y}_{NMR}$, was monitored as a function of the volume of water eluted through the dialysis ultrafiltration cell (Figure 3). It is clear that in the case of **1a**⊂β-CD[$\bar{n}_{Nom} = 10$] the cyclodextrins completely unthread during dialysis, whereas the threading ratio of **1**⊂β-CD[$\bar{n}_{Nom} = 10$] levels off at $\bar{y}_{NMR} = 1.1$. This proves that polyrotaxanes with naphthalene disulfonate endgroups are genuine rotaxanes, and that the great majority of chains have naphthalene stoppers at both ends. This experiment also demonstrates that β-cyclodextrin is able to slip over the carboxylic acid substituents along the polymer backbone. Similar experiments showed that polypseudorotaxane analogues of **2**⊂β-CD and **3**⊂β-CD, which lack the naphthalene endgroups, undergo slow unthreading, whereas those of **3**⊂α-CD do not unthread because α-cyclodextrin is too narrow to slip over the sulfonated stilbene units. We also tested the rate of unthreading in **1a**⊂β-CD as a function of the chain length, and showed that shorter chains unthread more rapidly. For example, when the experiment shown in Figure 3 was carried out with **1a**⊂β-CD[$\bar{n}_{Nom} = 4$] the threading ratio dropped to $\bar{y}_{NMR} < 0.1$ after only 2.5 L of water had been eluted.[25] Unthreading of higher molecular weight polypseudorotaxanes is accompanied by precipitation of the unthreaded polymer because the presence of the threaded cyclodextrin increases the solubility.

MALDI-TOF mass spectra: Figure 4 shows a negative ion MALDI-TOF MS of **1**⊂β-CD[$\bar{n}_{Nom} = 10$]. The spectrum consists of families of peaks with different numbers of threaded cyclodextrins (x) for each number of repeat units (n). It is interesting that some peaks are observed with a threading ratio greater than unity ($x > n + 1$) showing that each unsubstituted biphenyl is able to accommodate up to two cyclodextrin units. The space-filling model of **1**⊂β-CD[$n = 2$; $y = 1$] in Figure 4 (top) shows that at a threading ratio of unity, there is still space between the cyclodextrins for a second macrocycle to be accommodated on at least some repeat units. The number-average threading ratio increases with increasing number of repeat units, n, and is greater than unity when $n > 5$. The lower threading ratios for the shorter oligomers indicate that cyclodextrins are less easily accommodated near the naphthalene endgroups. Only one type of minor defect peak can be identified in the spectrum: peaks at $M + 152$ marked "▼" are assigned to chains with one extra homo-coupled biphenyl unit, from oxidative
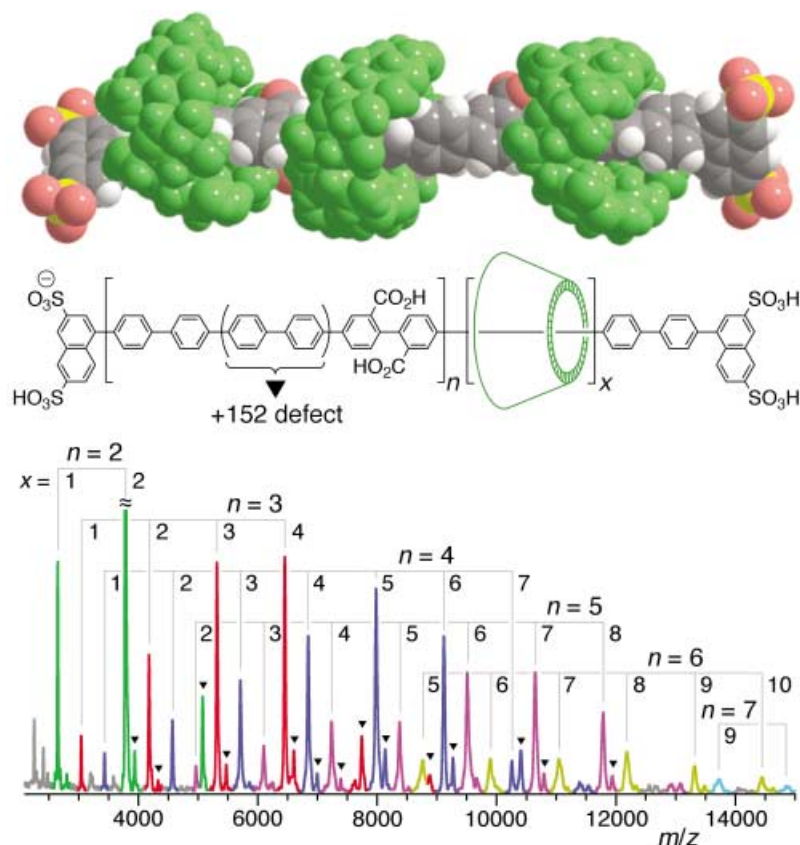
Figure 4. MALDI-TOF MS spectrum of $1 \subset \beta$-CD$[\bar{n}_{Nom} = 10]$, obtained with α-cyano-4-hydroxycinnamic acid as the matrix (negative mode). Triangles indicate molecular ions arising from chains with one defect as the result of an extra biphenyl unit. Colours indicate peaks from oligomers with $n = 2$ (green), $n = 3$ (red), $n = 4$ (blue), $n = 5$ (purple), $n = 6$ (mustard) and $n = 7$ (turquoise). The space-filling model (top) shows an energy-minimised structure of $1 \subset \beta$-CD$[n = 2; y = 1]$ with the cyclodextrin units shown in green (MM2 force field, CACHe 4.1.1).

coupling of **4a** by the Pd^{II} catalyst precursor. At first sight, the pattern of these defect peaks seems surprising: for example, there is a substantial $M+152$ defect peak at 5074 Da corresponding to $n = 2$, $x = 3$, but no significant parent peak for this n,x combination at 4922; similarly there is an defect orphan peak at 7737 Da corresponding to $n = 3$, $x = 5$, and the defect peak at 10400 Da corresponding to $n = 4$, $x = 7$ is larger than its parent. All these apparent anomalies make sense when one realises that an extra hydrophobic biphenyl unit is generally associated with an extra threaded β-cyclodextrin (so that it is really an $M+1287$ defect). We were unable to obtain satisfactory MALDI-TOF MS spectra of the PDV and PF polyrotaxanes, or of any of the reference polymers. The ability to transfer these polyrotaxanes into the gas phase by MALDI is remarkably sensitive to the details of the molecular structure. Even when good MALDI spectra are observed, they do not provide quantitative information on the molecular weight distribution because shorter chains are transferred into the gas phase more easily, as illustrated by the data in Figure 4 ($\bar{n}_{NMR} = 7.7$; $\bar{n}_{AUC} = 10.6$; $\bar{n}_{MALDI} = 3.6$).

Molecular weight determination: It is often difficult to determine the molecular weights of polyelectrolytes, and this was the case with our polyrotaxanes. Initially, we used polyacryl-

amide gel electrophoresis, relative to denatured protein markers, but this gave unrealistically high molecular weights,[17a] which is not surprising because the polyrotaxanes do not resemble proteins. Next, we turned to analytical GPC in a variety of solvent systems and calibrated with poly(ethylene glycol) standards. When a high ionic-strength eluant (400 mM LiNO$_3$, 1.5 mM LiOH, 1.0 mM Li$_2$CO$_3$) was used to suppress electrostatic interactions between polyelectrolyte chains, we obtained plausible results for $1 \subset \beta$-CD$[\bar{n}_{Nom} = 10]$ and $3 \subset \beta$-CD$[\bar{n}_{Nom} = 10]$ ($\bar{M}_w = 20$ and 13 kDa, respectively), but $2 \subset \beta$-CD$[\bar{n}_{Nom} = 10]$ and $3 \subset \alpha$-CD$[\bar{n}_{Nom} = 10]$ gave very long elution times corresponding to unrealistically low molecular weights ($\bar{M} < 1$ kDa); evidently, these materials adsorb onto the column material. The unthreaded polymers **1–3** completely adsorb onto the stationary phase under these conditions and gave no detectable peaks (UV detector, 330 nm). GPC with DMSO as the eluant also failed to give satisfactory results. Molecular weight determination by small angle neutron scattering (SANS) was also unsuccessful.[26]

Analytical ultracentrifugation (AUC) by equilibrium sedimentation[27] proved to be the most practical method of molecular weight determination. Although this technique is routinely used to determine the molecular weights of biopolymers, it is applied less often to synthetic polymers. When a polymer solution is centrifuged for about 20 h at an angular velocity of typically $1–3 \times 10^4$ rpm, equilibrium is reached between diffusion and sedimentation. A concentration gradient is established over the cell, which for a polydisperse solute with ideal behaviour is given by Equation (1),[27a, 28] where $c(r)$ and $\bar{M}_w(r)$ are the concentration and the weight-average molecular weight of the polymer as a function of r the radial distance (normally given in cm from the centre of rotation); $\bar{v}$ is the partial specific volume of the polymer, ρ is the density of the solution, ω is the rotor speed in radians per second, R is the gas constant and T is the temperature.

$$\frac{dc(r)}{dr} = \frac{\bar{M}_w(r)(1-\bar{v}\rho)\omega^2 r c(r)}{RT} \tag{1}$$

The weight-average molecular weight of the whole sample ($\bar{M}_w$) is obtained from the average slope of a plot of $\ln(c)$ versus r^2. In practice, the concentration gradient is

measured by UV/Vis absorption, assuming that the solute follows Beer's law, and c is substituted by absorbance (A), so $\bar{M}_w$ is determined with Equation (2).[27d]

$$\bar{M}_w(\mathrm{AUC}) = \frac{2RT}{(1-\bar{v}\rho)\omega^2}\left\langle\frac{d\ln A}{dr^2}\right\rangle \qquad (2)$$

All our polymers have high molar extinction coefficients, so low concentrations of polymer can be used (0.5–2 μg mL^{-1}), minimising non-ideal effects such as aggregation and electrostatic interactions between the polyelectrolyte chains. The experiments were carried out with a background salt ($I = 6.0$ mM) in order to further minimise non-ideal behaviour (see the Experimental Section). Figure 5 shows typi-
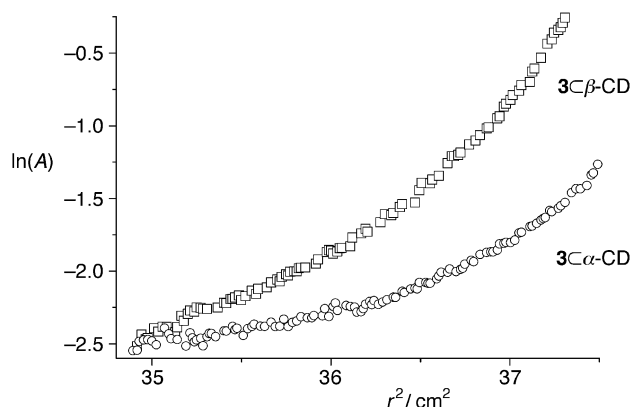

Figure 5. Sedimentation equilibrium profiles for the polyrotaxanes $3\subset\alpha$-CD and $3\subset\beta$-CD, both with a nominal degree of polymerisation of $\bar{n}_{Nom} = 10$. A is the optical density of the solution at radial distance r; $\lambda = 398$ nm; aqueous buffer: 1.25 mM LiOH, 1.58 mM Li$_2$CO$_3$; rotor speed = 15 000 rpm; $T = 20$°C; cell path length = 12 mm; stationary absorption at 398 nm, $A_0 = 0.25$.

cal AUC data for $3\subset\alpha$-CD and $3\subset\beta$-CD; here the steeper gradient for $3\subset\beta$-CD indicates a higher molecular weight, mainly on account of the higher threading ratio and the greater mass of β-CD.

The partial specific volumes of all seven polymers were determined densitometrically with the oscillating capillary technique.[29] This gave the values for $\bar{v}$ in Table 2, which were used to determine $\bar{M}_w(\mathrm{AUC})$ with Equation (2). The expected molecular masses $\bar{M}_w(\mathrm{calcd})$ were calculated from $\bar{n}_{Nom}$ by numerical integration of the Flory distribution of oligomers,[30] and experimental number-average degrees of polymerisation $\bar{n}_{AUC}$ were determined by calculating the mole ratio of **6** that would have given a Flory distribution with the observed $\bar{M}_w(\mathrm{AUC})$. There is generally good agreement between the experimental and calculated values of $\bar{M}_w$ and $\bar{n}$. The slightly low values of $\bar{n}_{AUC}$ for $2\subset\beta$CD and $3\subset\alpha$CD may reflect some accidental termination or incomplete coupling, whereas the high apparent $\bar{n}_{AUC}$ for polymers **1**--**3** are probably cased by the aggregation of these un-threaded polymers during the AUC measurements.

We also tested the efficiency of the Suzuki polymerisation by preparing a range of samples of $1\subset\beta$-CD with differ-

ent mole ratios of the mono-functional stopper **6** ($\bar{n}_{Nom} = 4$, 10, 15, 25 and 50) and comparing their molecular weights by AUC. The variation in $\bar{M}_w(\mathrm{AUC})$ with $\bar{n}_{Nom}$ is plotted in Figure 6. The straight line shows the ideal case, expected in the absence of accidental termination. At $\bar{n}_{Nom} = 4$, $\bar{M}_w(\mathrm{AUC})$ is higher than expected, because some short oligomers are lost during precipitation and dialysis, whereas,

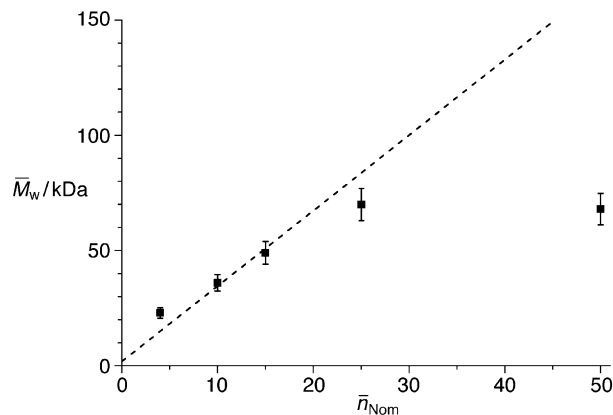Figure 6. Plot of $\bar{M}_w(\mathrm{AUC})$ versus $\bar{n}_{Nom}$ for $1\subset\beta$-CD. The straight line shows the ideal behaviour in the absence of accidental termination or fractionation during purification (assuming a threading ratio of $\bar{y} = 1.1$).

at high $\bar{n}_{Nom}$, the $\bar{M}_w(\mathrm{AUC})$ values become lower than predicted because accidental termination limits the molecular weight. $\bar{M}_w(\mathrm{AUC})$ reaches a limit of ≈ 70 kDa, which corresponds to an average chain length of approximately 20 repeat units. This implies that side-reactions limit the efficiency of the polymerisation reaction to ≈ 95%. The same conclusion was drawn from GPC analysis of these $1\subset\beta$-CD samples, although $\bar{M}_w$ values from GPC were systematically lower by a factor of ≈ 2.5. Extensive dialysis of "$1\subset\beta$-CD[$\bar{n}_{Nom} = 50$]" confirms that it is not a true polyrotaxane; β-cyclodextrin slowly unthreads and results in precipitation.

Absorption and fluorescence: The electronic absorption and emission spectra of these polyrotaxanes reveal how the conjugated π-system is affected by encapsulation. We have compared the behaviour in dilute aqueous solution[31] and in the solid state, as thin films spin-coated on silica substrates. The absorption and emission bands of the polyrotaxanes are generally sharper than those of the unencapsulated reference polymers. This can be attributed to reduced inter-chromophore interaction, and increased conformational homogeneity and rigidity in the polyrotaxanes. Examples of normalised absorption and emission spectra for the PF derivatives $2\subset\beta$-CD[$\bar{n}_{Nom} = 10$] and $2[\bar{n}_{Nom} = 10$] are shown in Figures 7 and 8. Here the sharper emission of the polyrotaxane enables vibrational structure to be observed in solution at room temperature. At low temperature (e.g. 10 K, Figure 8) the vibrational structure is beautifully resolved in the solid-state emission spectra of both the polyrotaxane and the reference polymer. Cyclodextrin encapsulation increases the intensity of the 0–0 band, relative to that of the 0–1 band; this is seen most clearly in the low-temperature spectra, but is also evi-
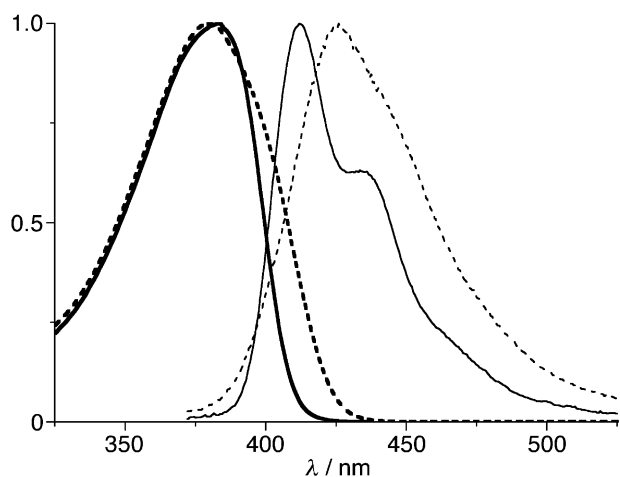
Figure 7. Normalised absorption spectra (bold) and emission spectra (plain) of $2 \subset \beta$-CD (——) and **2** (-----) in aqueous solution (both $\bar{n}_{\text{Nom}}$ = 10; 1.66 mM LiOH, 2.11 mM Li_2CO_3 aqueous buffer, pH 9; emission spectra with excitation at 361 nm).
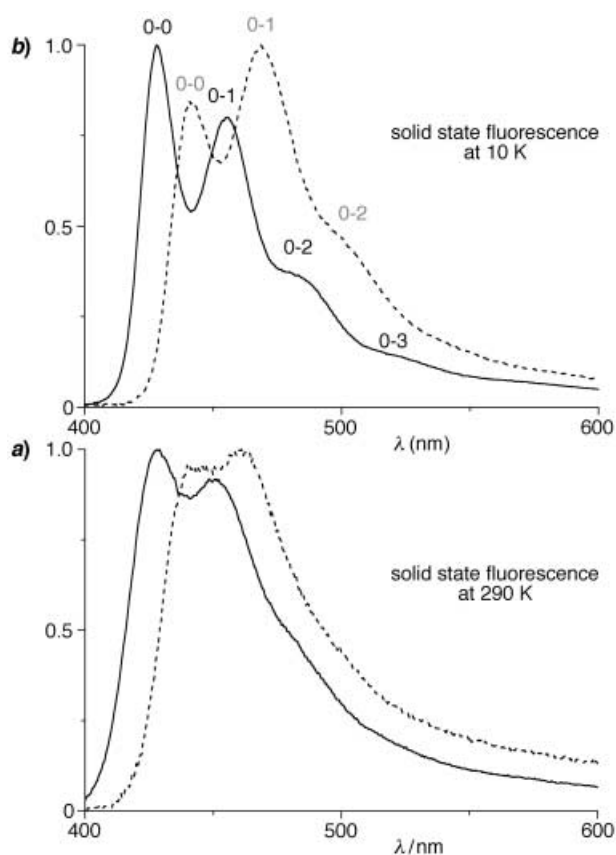

Figure 8. Normalised emission spectra of $2 \subset \beta$-CD (——) and **2** (-----) in the solid state at a) 290 K and b) at 10 K (both $\bar{n}_{\text{Nom}}$ = 10).

dent at 290 K. According to the Franck–Condon principle, this change in band shape implies that the change in geometry between the excited state and the ground state is smaller in the case of the polyrotaxane. In other words, encapsulation increases the rigidity of the π system.

The wavelengths of the absorption and emission maxima increase in the order PPP < PF < PDV, reflecting the extent of conjugation in their conjugated polymer backbones.[32] For each polymer backbone, the emission spectra of the polyrotaxane are shifted to shorter wavelength relative to the reference polymer (Table 3). The smaller Stokes shift in the polyrotaxanes is partly a result of the increased 0–0:0–1 intensity ratio; however in those spectra where it is resolved, the 0–0 peak is also blue-shifted in the case of the polyrotaxanes, implying that encapsulation reduces the amount of re-organisation in the excited state. The absorption spectra are less affected by encapsulation.

The fluorescence quantum yields in Table 3 show that the polyrotaxanes exhibit enhanced fluorescence efficiencies, both in solution and in the solid state. A similar effect was observed in the analogous [2]rotaxanes[8] and can be attributed to the reduced flexibility of the encapsulated π-system, as well as to reduced solvent-quenching (in dilute solution) and reduced aggregation (in the solid state). It is interesting that $3 \subset \beta$-CD has a significantly higher fluorescence quantum yield than $3 \subset \alpha$-CD, both in solution and in the solid state, whereas in the [2]rotaxanes α-cyclodextrin gives a greater fluorescence enhancement. The higher fluorescence efficiency of the β-cyclodextrin polyrotaxane is probably caused by its higher threading ratio (Table 2). Light-emitting diodes have been fabricated from all seven of these polymers and the electroluminescence quantum yields of the polyrotaxanes are found to be enhanced more strongly than their fluorescence quantum yields.[17b] The details of these electroluminescence results will be reported shortly.

Conclusion

An efficient preparation of water-soluble conjugated polyrotaxanes, based on poly-*para*-phenylene, polyfluorene and poly-*para*-diphenylenevinylene, has been developed. Polyrotaxane synthesis is accomplished by polymerisation of cyclodextrin-bound monomers by means of an aqueous Suzuki coupling. ^{1}H NMR shows that the polymer chains are efficiently threaded with cyclodextrins, with approximately one cyclodextrin per unsubstituted biphenyl, fluorene or stilbene unit. This cyclodextrin-loading leaves some regions of the conjugated backbone exposed, which probably facilitates charge-transport through bulk polyrotaxanes.[17b] The naphthalene disulfonate endgroups are bulky enough to prevent the cyclodextrins from unthreading, even after extensive dialysis. MALDI-TOF mass spectra of PPP-based polyrotaxanes show the expected pattern of molecular ions for polyrotaxanes with different lengths and different numbers of threaded cyclodextrins, and confirm the presence of some homo-coupled biphenyl defects. Analytical ultracentrifugation gave weight-average molecular weights which compare well with those predicted from the polymerisation stoichiometries, for polymers with up to 20 repeat units (which corresponds to 84 *para*-phenylene residues). The fluorescence spectra of the polyrotaxanes show that the presence of the cyclodextrins reduces the flexibility of the π system, as manifested by the sharper emission spectra, the increased 0–0

Table 3. Wavelengths of the absorption and emission maxima and photoluminescence quantum yields.[a]

Polymer	Solution spectra			Solid-state thin-film spectra		
	λ_{abs} [nm]	λ_{em} [nm]	$\Phi_{solution}$	λ_{abs} [nm]	λ_{em} [nm]	Φ_{film}
$1 \subset \beta$-CD	338	390	0.65	337	433	0.15
$2 \subset \beta$-CD	383	412	0.74	378	428	0.072
$3 \subset \alpha$-CD	397	447	0.18	390	510	0.11
$3 \subset \beta$-CD	396	444	0.26	391	509	0.17
1	338	395	0.31	340	440	0.12
2	380	424	0.19	384	442	0.048
3	400	478	0.10	395	540	0.043

[a] Solution spectra were recorded in a 1.66 mM LiOH, 2.11 mM Li$_2$CO$_3$ aqueous buffer (pH 9) at concentrations of ≈ 1 μM for absorption and 0.1 μM for emission. The estimated errors in the solution and solid-state quantum yields ($\Phi_{solution}$ and Φ_{film}) are less than 10%. All polymers are $\bar{n}_{Nom} = 10$.

Franck–Condon factors, and the higher fluorescence quantum yields, both in solution and in the solid state. The thorough chemical characterisation of these insulated molecular wires prepares the way for a full investigation of their solid-state physics and semiconducting properties.

Experimental Section

Compound 1$\subset\beta$-CD[$\bar{n}_{Nom} = 10$]: A two-necked flask was charged with diiodide **4a** (100 mg, 0.20 mmol), diboronic ester **5a** (71 mg, 0.24 mmol), 1-iodonaphthalene-3,6-disulfonate disodium salt (**6**, 19 mg, 0.040 mmol), β-cyclodextrin (929 mg, 0.818 mmol), [Pd(OAc)$_2$] (4.5 mg, 0.020 mmol), and Li$_2$CO$_3$ (90 mg, 1.2 mmol) and N$_2$-saturated water (7 mL) was added by syringe. The mixture was stirred over night at 85°C. The colour changed from reddish brown to black during the first hour. The solution was diluted with water (10 mL) and passed through a 0.22 μm filter (cellulose ester membrane). The solution was acidified to pH 1 with HCl (2 M aq.) to give a gelatinous precipitate, which was separated by centrifugation (5 min at 4000 rpm). The crude product was redissolved in aqueous Li$_2$CO$_3$ (40 mL, 90 mM, pH 10) and stirred with NaCN (50 mg, 1.0 mmol) **[Toxic!]** for 5 h. During this time, the colour changed from dark brown to pale yellow. The product was further purified from low-molecular weight material by ultrafiltration (polysulfone membrane; NMWCO 5 kDa), then passed through a 0.22 μm filter and evaporated to yield 1$\subset\beta$-CD[$\bar{n}_{Nom} = 10$] (200 mg, 54%) as a pale beige film. ^{1}H NMR (250 MHz, D$_2$O): δ = 8.6–8.4 (4H), 8.4–7.2 ([14 + 14n]H; n = 7.7±1), 5.2–4.8 (7xH), 4.2–2.9 ppm (42xH; x = 8.5±1); ^{13}C NMR (125 MHz, D$_2$O): δ = 178, 142–134, 131, 128–124, 102, 81, 74, 73, 60 ppm; UV (H$_2$O): λ_{max} = 211, 338 nm; elemental analysis calcd[33] (%) for C$_{774}$H$_{953}$O$_{449}$S$_4$Li$_{25}$·53H$_2$O: C 49.77, H 5.71, Li 0.91; found: C 49.77, H 5.71, Li 0.92, B < 0.1, I < 0.1, Pd < 0.02.

Compound 2$\subset\beta$-CD[$\bar{n}_{Nom} = 10$]: This polyrotaxane was prepared by the same procedure as 1$\subset\beta$-CD[$\bar{n}_{Nom} = 10$] but with diiodide **4b** (122 mg, 0.218 mmol), diboronic ester **5b** (80 mg, 0.26 mmol), 1-iodonaphthalene-3,6-disulfonate disodium salt (**6**, 20 mg, 0.044 mmol), β-cyclodextrin (989 mg, 0.872 mmol), [Pd(OAc)$_2$] (4.9 mg, 0.022 mmol), Li$_2$CO$_3$ (97 mg, 1.3 mmol) and NaCN (50 mg, 1.0 mmol) **[Toxic!]**. 2$\subset\beta$-CD[$\bar{n}_{Nom} = 10$] (340 mg, 86%) was obtained as a pale beige film. ^{1}H NMR (250 MHz, D$_2$O): δ = 8.6–8.4 (4H), 8.4–7.2 ([12 + 12n]H; n = 10.4±1), 5.2–4.8 (7xH), 4.3–2.9 ([2 + 2n + 42x]H, x = 11.5±1), 2.45 ([4 + 4n]H), 1.45 ppm ([4 + 4n]H); ^{13}C NMR (125 MHz, D$_2$O): δ = 140–142, 120–128, 102.2, 81.2, 73.7, 72.5, 60.0 ppm; UV (H$_2$O): λ_{max} = 215, 235, 383 nm; elemental analysis calcd[33] (%) for C$_{682}$H$_{842}$O$_{367}$S$_4$Li$_{20}$·61H$_2$O: C 50.33, H 5.97, Li 0.84; found: C 50.36, H 6.14, Li 0.40, B < 0.1.

Compound 3$\subset\alpha$-CD[$\bar{n}_{Nom} = 10$]: This polyrotaxane was prepared by the same procedure as 1$\subset\beta$-CD[$\bar{n}_{Nom} = 10$], but with diiodide **4c** (133 mg, 0.208 mmol), diboronic ester **5c** (320 mg, 0.250 mmol), 1-iodonaphthalene-3,6-disulfonate disodium salt (**6**, 19 mg, 0.040 mmol), α-cyclodextrin (810 mg, 0.832 mmol), [Pd(OAc)$_2$] (4.7 mg, 0.021 mmol), Li$_2$CO$_3$ (92 mg, 1.2 mmol) and NaCN (50 mg, 1.0 mmol) **[Toxic!]**. The PDV-based materials were not precipitated with acid. The excess cyclodextrin, as well as

low molecular weight material, was removed by ultrafiltration. 3$\subset\alpha$-CD[$\bar{n}_{Nom} = 10$] (230 mg, 66%) was obtained as a pale yellow film. ^{1}H NMR (250 MHz, D$_2$O): δ = 8.6–8.4 (4H), 8.6–6.7 ([16 + 18n]H; n = 7.9±1), 5.2–4.8 (6xH), 4.2–2.9 ppm (36xH; x = 7.1±1); ^{13}C NMR (125 MHz, D$_2$O): δ = 138–142, 124–130, 102.0, 81.2, 73.6, 72.2, 71.8, 59.8 ppm; UV (H$_2$O): λ_{max} = 205, 234, 397 nm; elemental analysis calcd[33] (%) for C$_{586}$H$_{693}$O$_{323}$S$_{21}$Li$_{21}$·56H$_2$O: C 47.76, H 5.51, Li 1.00; found: C 47.79, H 5.71, B < 0.1.

Compound 3$\subset\beta$-CD[$\bar{n}_{Nom} = 10$]: This polyrotaxane was prepared by the same procedure as 3$\subset\alpha$-CD[$\bar{n}_{Nom} = 10$], but with diiodide **4c** (83 mg, 0.13 mmol), diboronic ester **5c** (50 mg, 0.16 mmol), 1-iodonaphthalene-3,6-disulfonate disodium salt (**6**, 12 mg, 0.026 mmol), β-cyclodextrin (703 mg, 0.620 mmol), [Pd(OAc)$_2$] (3.1 mg, 0.014 mmol), Li$_2$CO$_3$ (61 mg, 0.83 mmol) and NaCN (50 mg, 1.0 mmol) **[Toxic!]**. 3$\subset\beta$-CD[$\bar{n}_{Nom} = 10$] (160 mg, 48%) was obtained as a pale yellow film. ^{1}H NMR (250 MHz, D$_2$O): δ = 8.6–8.4 (4H), 8.6–6.3 ([16 + 18n]H; n = 7.7±1), 5.2–4.8 (7xH), 4.2–2.9 ppm (42xH, x = 12±1); ^{13}C NMR (125 MHz, D$_2$O): δ = 138–142, 124–130, 102.0, 80.7, 73.3, 72.2, 60.2 ppm; UV (H$_2$O): λ_{max} = 205, 234, 397 nm; elemental analysis calcd[33] (%) for C$_{1177}$H$_{1601}$O$_{769}$S$_{27}$Li$_{27}$·86H$_2$O: C 46.15, H 5.83, Li 0.60; found: C 46.17, H 5.29, Li 0.64, B < 0.1.

Compound 1[$\bar{n}_{Nom} = 10$]: This polymer was prepared analogously to 1$\subset\beta$-CD[$\bar{n}_{Nom} = 10$], but with diiodide **4a** (168 mg, 0.340 mmol), diboronic ester **5a** (120 mg, 0.408 mmol), 1-iodonaphthalene-3,6-disulfonate disodium salt (**6**, 31 mg, 0.068 mmol), [Pd(OAc)$_2$] (7.6 mg, 0.034 mmol), Li$_2$CO$_3$ (151 mg, 2.04 mmol) and NaCN (80 mg, 1.6 mmol) **[Toxic!]**. 1[$\bar{n}_{Nom} = 10$] (87 mg, 45%) was obtained as a pale beige film. ^{1}H NMR (250 MHz, D$_2$O): δ=8.6–8.4 (4H), 8.4–6.4 ([14 + 14n]H; n = 11±2); ^{13}C NMR (125 MHz, D$_2$O): δ = 178, 142–136, 131, 130–124; UV (H$_2$O): λ_{max} = 208, 337 nm; anal. calcd[33] (%) for C$_{461}$H$_{249}$O$_{78}$S$_4$Li$_{37}$·80H$_2$O: C 62.37, H 4.66, Li 2.90; found: C 62.77, H 4.62, Li 2.91, B < 0.1, Pd < 0.02.

Compound 2[$\bar{n}_{Nom} = 10$]: This polymer was prepared analogously to 1$\subset\beta$-CD[$\bar{n}_{Nom} = 10$], but with diiodide **4b** (184 mg, 0.327 mmol), diboronic ester **5b** (120 mg, 0.392 mmol), 1-iodonaphthalene-3,6-disulfonate disodium salt (**6**, 30 mg, 0.065 mmol), [Pd(OAc)$_2$] (7.3 mg, 0.033 mmol), Li$_2$CO$_3$ (145 mg, 1.96 mmol) and NaCN (80 mg, 1.6 mmol) **[Toxic!]**. No colour change was observed after stirring for 1 h with NaCN. After heating the solution for 1 min at 60°C, the dark brown colour disappeared readily. The solution was stirred for an additional 18 h at room temperature. 2[$\bar{n}_{Nom} = 10$] (177 mg, 97%) was obtained as a light brownish green film. ^{1}H NMR (250 MHz, D$_2$O): δ = 9.0–7.3 ([16 + 12n]H), 2.5–0.5 ppm ([10 + 10n]H); ^{13}C NMR (125 MHz, D$_2$O): δ = 185, 135–150, 120–130, 30–40 ppm; UV (H$_2$O): λ_{max} = 212, 379 nm; elemental analysis calcd[33] (%) for C$_{740}$H$_{504}$O$_{100}$S$_4$Li$_{48}$·346H$_2$O: C 50.20, H 6.81, Li 1.89; found: C 50.10, H 5.47, Li 1.59, B < 0.1.

Compound 3[$\bar{n}_{Nom} = 10$]: This polymer was prepared analogously to 3$\subset\alpha$-CD[$\bar{n}_{Nom} = 10$], but with diiodide **4c** (83 mg, 0.13 mmol), diboronic ester **5c** (50 mg, 0.16 mmol), 1-iodonaphthalene-3,6-disulfonate disodium salt **6** (13 mg, 0.026 mmol), [Pd(OAc)$_2$] (3.1 mg, 0.014 mmol), Li$_2$CO$_3$ (61 mg, 0.83 mmol) and NaCN (50 mg, 1.0 mmol) **[Toxic!]**. 3[$\bar{n}_{Nom} = 10$] (45 mg, 57%) was obtained as a pale yellow film. ^{1}H NMR (250 MHz, D$_2$O): δ = 8.8–6.7 ppm ([18 + 18n]H); ^{13}C NMR (125 MHz, D$_2$O): δ = 141, 137, 130–120 ppm; UV (H$_2$O): λ_{max} = 204, 400 nm; elemental analysis calcd[33] (%) for C$_{376}$H$_{240}$O$_{85}$S$_{28}$Li$_{28}$·97H$_2$O: C 50.26, H 4.88, Li 2.20; found: C 50.36, H 5.44, Li 1.56, B < 0.1.

Mass spectra: of 1$\subset\beta$-CD were recorded on a Micromass Tof Spec 2E MALDI-TOF mass spectrometer (with a nitrogen laser operating at 337 nm). α-Cyano-4-hydroxycinnamic acid was used as a matrix. A 5 mg mL^{-1} solution of polyrotaxane in water was mixed 1:1 with a 10 mg mL^{-1} solution of the matrix in water/acetonitrile (70:30). 1.2 μL of this mixture was applied to the target plate and allowed to dry. Negative ion spectra were obtained by running the spectrometer in the linear

mode, with a laser power of typically 50% (course)/40–45% (fine), in combination with a pulse voltage of 1200 V. Smoothing of the acquired spectra revealed signals corresponding to high molecular weight material.

Dialysis: was carried out in an Amicon 8200 ultrafiltration stirred cell (200 mL) and polysulfone membranes (NMWCO 5 kDa). At least 3 L of water was eluted through the ultrafiltration cell for each polymer sample and under 4 bar nitrogen pressure.

Palladium analysis: A known mass of polymer (≈ 10 mg) was dissolved in hot, freshly prepared, piranha solution (4 mL, 7:3 conc. sulfuric acid/35% aq. H_2O_2) in a 10 mL volumetric flask. Water (≈ 6 mL) was added in order to obtain the desired volume (10 mL) and the solution was homogenised by shaking the flask. The analysis was carried out on this solution in a Thermo Jarrell Ash Atom Scan 16 spectrometer with inductive argon plasma coupling.

Gel permeation chromatography: (GPC) was carried out on a Polymer Laboratories instrument, equipped with refractive index and UV/Vis detectors. Aqueous GPC was performed with a basic buffer (400 mm $LiNO_3$, 1.5 mm $LiOH$, 1.0 mm Li_2CO_3) as the eluant on PLaquagel-OH-30 8 µm and PLaquagel-OH-40 8 µm columns (300×7.5 mm), calibrated with poly(ethylene oxide) standards. 4-Acetylamino-5-hydroxy-naphthalene-2,7-disulfonic acid was used as a flow-rate marker. Organic GPC was performed with DMSO as the eluant on PLgel 5 µm MIXED-D columns (300×7.5 mm), calibrated with polystyrene standards.

Analytical ultracentrifugation: Weight-average molecular weights were determined by sedimentation equilibrium at 20°C in a Beckman Coulter XLA Analytical Ultracentrifuge, equipped with an AN 60 rotor and a UV/Vis detection system. The samples were prepared by dissolving polymer in aqueous buffer (1.25 mm $LiOH$/1.58 mm Li_2CO_3, pH 8.5). Each sample was spun at three different initial loading concentrations, typically in the range 0.5–2 µg mL^{-1}. Rotor speeds were chosen in the range 15 000–20 000 rpm for the polyrotaxanes, and 25 000–30 000 rpm for the reference polymers; at higher rotor speeds, high molecular weight fractions are deposited on the base of the cell resulting in a decrease in the apparent molecular weight. Concentration profiles were monitored by measuring the absorbance across the cell at λ_{max} of the high-wavelength absorption bands of the polymers (338 nm for $1 \subset \beta$-CD and **1**, 384 nm for $2 \subset \beta$-CD and **2**), and 398 nm for $3 \subset \alpha$-CD, $3 \subset \beta$-CD, and **3**). No residual (baseline) absorption was observed after equilibrating at 48 000 rpm. Molecular weight averages were obtained from the average slopes of $\ln A$ versus r^2 by means of Equation (2).[27] No dependence of the molecular weight on either rotor speed or loading concentration was observed. Partial specific volumes ($\bar{v}$) were determined densitometrically[29] at the National Centre for Macromolecular Hydrodynamics (Nottingham, UK), in an Anton Paar DMA 02C Precision Density Meter. All measurements were carried out at 20°C.

Photophysical measurements: UV/Vis and luminescence spectra were recorded on Perkin Elmer Lambda 20 and Fluoromax-2 spectrometers. The luminescence quantum yields of the polymers (Φ_A) in basic aqueous solution (1.66 mm $LiOH$/2.11 mm Li_2CO_3, pH 9) were determined relative to the fluorescence quantum yield (Φ_B) of a solution of quinine hemisulfate salt in 0.5 m H_2SO_4 as a standard ($\Phi_B = 0.546$), according to $\Phi_A = [(A_B F_A n_A^2)/(A_A F_B n_B^2)]\Phi_B$, where A, F and n are absorbance, integrated fluorescence intensity and refractive index, respectively. The refractive indices of solutions of polymer and standard were assumed to be equal. In a typical experiment, the fluorescence intensity of the sample and the standard was measured at four different concentrations at low optical density ($A < 0.1$). Φ_A was subsequently obtained from the slopes of plots of F versus A. Solid-state fluorescence spectra were measured by means of excitation with UV lines (355–365 nm) of an argon ion laser. Variable-temperature spectra were recorded by placing the sample in a continuous-flow helium cryostat capable of cooling to around 9 K, under a pressure of ≈ 8 mbar of helium. Emission spectra were recorded on an Oriel Instaspec IV spectrometer at a fixed geometry such that the relative photoluminescence intensity at different temperatures can be compared. Solid-state fluorescence quantum yields were measured with an integrating sphere

[1] J. H. Burroughes, D. D. C. Bradley, A. R. Brown, R. N. Marks, K. Mackay, R. H. Friend, P. L. Burn, A. B. Holmes, *Nature* **1990**, *347*, 539–541; G. Gustafsson, Y. Cao, G. M. Treacy, F. Klavetter, N. Colaneri, A. J. Heeger, *Nature* **1992**, *357*, 477–479.

[2] H. Sirringhaus, N. Tessler, R. H. Friend, *Science* **1998**, *280*, 1741–1744.

[3] N. S. Sariciftci, D. Braun, C. Zhang, V. I. Srdanov, A. J. Heeger, G. Stucky, F. Wudl, *Appl. Phys. Lett.* **1993**, *62*, 585–587; M. Granström, K. Petritsch, A. C. Arias, A. Lux, M. R. Andersson, R. H. Friend, *Nature* **1998**, *395*, 257–260.

[4] R. J. O. M. Hoofman, M. P. de Haas, L. D. A. Siebbeles, J. M. Warman, *Nature* **1998**, *392*, 54–56.

[5] H. Sirringhaus, P. J. Brown, R. H. Friend, M. M. Nielsen, K. Bechgaard, B. M. W. Langeveld-Voss, A. J. H. Spiering, R. A. J. Janssen, E. W. Meijer, P. Herwig, D. M. de Leeuw, *Nature* **1999**, *401*, 685–688.

[6] J. Cornil, D. A. dos Santos, X. Crispin, R. Silbey, J. L. Brédas, *J. Am. Chem. Soc.* **1998**, *120*, 1289–1299.

[7] M. R. Craig, M. G. Hutchings, T. D. W. Claridge, H. L. Anderson, *Angew. Chem.* **2001**, *113*, 1105–1108; *Angew. Chem. Int. Ed.* **2001**, *40*, 1071–1074.

[8] C. A. Stanier, M. J. O'Connell, W. Clegg, H. L. Anderson, *Chem. Commun.* **2001**, 493–494 and 787.

[9] T. Bein, P. Enzel, *Angew. Chem.* **1989**, *101*, 1737–1739; *Angew. Chem. Int. Ed. Engl.* **1989**, *28*, 1692–1694.

[10] S. Anderson, R. T. Aplin, T. D. W. Claridge, T. Goodson, A. C. Maciel, G. Rumbles, J. F. Ryan, H. L. Anderson, *J. Chem. Soc. Perkin Trans. 1* **1998**, 2383–2397.

[11] J. Buey, T. M. Swager, *Angew. Chem.* **2000**, *112*, 622–626; *Angew. Chem. Int. Ed.* **2000**, *39*, 608–612; J.-P. Sauvage, J.-M. Kern, G. Bidan, B. Divisia-Blohorn, P.-L. Vidal, *New J. Chem.* **2002**, *26*, 1287–1290.

[12] T. Shimomura, T. Akai, T. Abe, K. Ito, *J. Chem. Phys.* **2002**, *116*, 1753–1756; K. Yoshida, T. Shimomura, K. Ito, R. Hayakawa, *Langmuir* **1999**, *15*, 910–913; H. Okumura, Y. Kawaguchi, A. Harada, *Macromol. Rapid Commun.* **2002**, *23*, 781–785.

[13] V. S.-Y. Lin, D. R. Radu, M.-K. Han, W. Deng, S. Kuroki, B. H. Shanks, M. Pruski, *J. Am. Chem. Soc.* **2002**, *124*, 9040–9041; D. J. Cardin, S. P. Constantine, A. Gilbert, A. K. Lay, M. Alvaro, M. S. Galletero, H. Garcia, F. Marquez, *J. Am. Chem. Soc.* **2001**, *123*, 3141–3142; D. J. Cardin, *Adv. Mater.* **2002**, *14*, 553–563; C.-G. Wu, T. Bein, *Science* **1994**, *264*, 1757–1759; T.-Q. Nguyen, J. Wu, S. H. Tolbert, B. J. Schwartz, *Adv. Mater.* **2001**, *13*, 609–611.

[14] J. Stahl, J. C. Bohling, E. B. Bauer, T. B. Peters, W. Mohr, J. M. Martín-Alvarez, F. Hampel, J. A. Gladysz, *Angew. Chem.* **2002**, *114*, 1951–1957; *Angew. Chem. Int. Ed.* **2002**, *41*, 1871–1876.

[15] A. P. H. J. Schenning, J.-D. Arndt, M. Ito, A. Stoddart, M. Schreiber, P. Siemsen, R. E. Martin, C. Boudon, J.-P. Gisselbrecht, M. Gross, V. Gramlich, F. Diederich, *Helv. Chim. Acta* **2001**, *84*, 296–334; A. D. Schlüter, J. P. Rabe, *Angew. Chem.* **2000**, *112*, 860–880; *Angew. Chem. Int. Ed.* **2000**, *39*, 864–883; P. R. L. Malenfant, J. M. J. Fréchet, *Macromolecules* **2002**, *35*, 3634–3640.

[16] A polyrotaxane is defined as a supramolecular structure with a polymer backbone threaded through several macrocyclic units. There is no covalent link between the macrocycles and the polymer chain,

but the macrocycles are unable to slip off the ends of the polymer on account of the presence of bulky terminal units.

[17] For preliminary communications on the synthesis and electroluminescence of these polyrotaxanes, see: a) P. N. Taylor, M. J. O'Connell, L. A. McNeill, M. J. Hall, R. T. Aplin, H. L. Anderson, *Angew. Chem.* **2000**, *112*, 3598–3602; *Angew. Chem. Int. Ed.* **2000**, *39*, 3456–3460; b) F. Cacialli, J. S. Wilson, J. J. Michels, C. Daniel, C. Silva, R. H. Friend, N. Severin, P. Samorì, J. P. Rabe, M. J. O'Connell, P. N. Taylor, H. L. Anderson, *Nat. Mater.* **2002**, *1*, 160–164. The synthesis of a β-cyclodextrin-threaded poly(azomethine) polyrotaxane has been reported recently: D. Nepal, S. Samal, K. E. Geckeler, *Macromolecules* **2003**, *36*, 3800–3802; A. Farcus, M. Grigoras, *J. Optoelectron. Adv. Mater.* **2000**, *2*, 525–530; A. Farcus, M. Grigoras, *Polymer Int.* **2003**, *52*, 1312–1320.

[18] F. M. Raymo, J. F. Stoddart, *Chem. Rev.* **1999**, *99*, 1643–1663; K. Kim, *Chem. Soc. Rev.* **2002**, *31*, 96–107; A. Harada, *Acc. Chem. Res.* **2001**, *34*, 456–464.

[19] A. Suzuki, *J. Organomet. Chem.* **1999**, *576*, 147–168; M. B. Goldfinger, K. B. Crawford, T. M. Swager, *J. Am. Chem. Soc.* **1997**, *119*, 4578–4593; C. Kowitz, G. Wegner, *Tetrahedron* **1997**, *53*, 15553–15574; N. Miyaura, A. Suzuki, *Chem. Rev.* **1995**, *95*, 2457–2483; J. C. Ostrowski, M. R. Robinson, A. J. Heeger, G. C. Bazan, *Chem. Commun.* **2002**, 784–785.

[20] The synthesis and characterisation of compounds **4a–c**, **5a–c** and **6** are detailed in the Supporting Information to this article.

[21] N. A. Bumagin, V. V. Bykov, *Tetrahedron* **1997**, *53*, 14437–14450; T. I. Wallow, B. M. Novak, *J. Org. Chem.* **1994**, *59*, 5034–5037; A. D. Child, J. R. Reynolds, *Macromolecules* **1994**, *27*, 1975–1977; S. Kim, J. Jackiw, E. Robinson, K. S. Schanze, J. R. Reynolds, J. Baur, M. F. Rubner, D. Boils, *Macromolecules* **1998**, *31*, 964–974.

[22] M. Moreno-Mañas, M. Pérez, R. Pleixats, *J. Org. Chem.* **1996**, *61*, 2346–2351; K. A. Smith, E. M. Campi, W. R. Jackson, S. Marcuccio, C. G. M. Naeslund, G. B. Deacon, *Synlett* **1997**, 131–132.

[23] J. C. Nelson, J. K. Young, J. S. Moore, *J. Org. Chem.* **1996**, *61*, 8160–8168.

[24] We were unable to detect iodine or boron in these polymers by elemental analysis (<0.1%) demonstrating the absence of unreacted boronic acid or aryl iodide endgroups.

[25] The rate of unthreading in α-cyclodextrin/poly(imine) pseudorotaxanes also decreases with decreasing chain length: G. Wenz, B. Keller, *Angew. Chem.* **1992**, *104*, 201–203; *Angew. Chem. Int. Ed. Engl.* **1992**, *31*, 197–199; W. Herrmann, B. Keller, G. Wenz, *Macromolecules* **1997**, *30*, 4966–4972.

[26] Small-angle neutron scattering measurements (using the LOQ instrument, Rutherford Appleton Laboratory, UK) were performed on **1**⊂β-CD[$\bar{n}_{Nom}$ = 10] and **1**[$\bar{n}_{Nom}$ = 10] in D$_2$O by Dr D. G. Bucknall (Department of Materials, University of Oxford), with momentum transfer range 0.009–0.25 Å^{-1}. Scattering data from 1.25, 2.5 and 5% wt./wt. solutions all indicated concentration dependent aggregation behaviour, as observed by excess scattering at momentum transfer values of approximately 0.03, 0.05 and 0.07 Å^{-1}, respectively. This non-ideal behaviour prevents determination of single-chain molecular dimensions; however, further analysis may allow extraction of characteristic length scales and apparent average molecular weights of aggregates.

[27] a) M. Wales, *J. Phys. Colloid Chem.* **1948**, *52*, 235–246; b) C. Tanford, *Physical Chemistry of Macromolecules*, Wiley, New York, **1961**; c) J. M. Creeth, R. H. Pain, *Prog. Biophys. Mol. Biol.* **1967**, *17*, 217–287; d) *Analytical Ultracentrifugation in Biochemistry and Polymer Science* (Eds: S. E. Harding, A. J. Rowe, J. C. Horton), Royal Society of Chemistry, Cambridge, **1992**; e) D. Schubert, C. Tziatzios, P. Schuck, U. S. Schubert, *Chem. Eur. J.* **1999**, *5*, 1377–1383.

[28] For systems containing a polyelectrolyte with a background salt, it is usually more accurate to utilise the density increment at constant chemical potential of diffusible components, $(d\rho/dc)_\mu$, instead of the buoyancy factor, $(1-\bar{v}\rho)$, due to the Donnan effect (see: Budd, P. M. in *Analytical Ultracentrifugation in Biochemistry and Polymer Science* (Eds.: S. E. Harding, A. J. Rowe, J. C. Horton), Royal Society of Chemistry: Cambridge, **1992**, pp.593–608). However, we assume variations in $\bar{v}$ across the cell at sedimentation equilibrium to be small and not to be contributing significantly to the experimental error.

[29] O. Kratky, H. Leopold, H. Stabinger, *Methods in Enzymology* **1973**, *27*, 98–110.

[30] Predicted $\bar{M}_w$(calcd) values were obtained from the mole fraction of mono-iodide **6** used in the polymerisation reactions by numerical integration of the Flory distribution of oligomers, assuming that all aryl iodide units react at equal rate, that Suzuki coupling goes to completion and that there are no accidental termination reactions.

[31] The fluorescence quantum yields were determined in aqueous solution at pH 9 (1.66 mM LiOH, 2.11 mM Li$_2$CO$_3$), which guaranteed complete deprotonation of the polymer chains. Under more acidic conditions, the quantum yields proved to be sensitive to pH, but no changes were observed above pH 8. Fluorescence quantum yields are independent of ionic strength up to 2 M NaCl.

[32] M. Fukuda, K. Sawada, K. Yoshino, *J. Polym. Sci. Polym. Chem. Ed. J. Polym. Sci. Polym. Chem.* **1993**, *31*, 2465–2471.

[33] Elemental analyses are compared with formulae calculated from $\bar{y}_{NMR}$ and $\bar{n}_{AUC}$ (Table 2).